

Original Research Paper

# Uncertainty Assessment for the Buckling Analysis of Glass Columns with Random Parameters

<sup>1</sup>Mohammad Momeni and <sup>2\*</sup>Chiara Bedon

<sup>1</sup>Shiraz University of Technology, Shiraz, Iran

<sup>2</sup>University of Trieste, Trieste, Italy

## Article history

Received: 16-10-2020

Revised: 12-12-2020

Accepted: 21-12-2020

Corresponding Author:

Chiara Bedon

University of Trieste, Trieste,

Italy

E-mail: chiara.bedon@dia.units.it

**Abstract:** Load-bearing elements composed of glass, as known, are often susceptible to buckling collapse mechanisms. This intrinsic characteristic (and thus potential limitation for design) typically derives from the use of relatively small thicknesses to cover large spans and surfaces, thus resulting in a multitude of columns, beams, or plates that are characterized by high slenderness. In the literature, accordingly, several and design propositions support of the definition of efficient calculation models to capture the typical buckling response of glass elements variably shaped, sized, restrained and loaded. In this study, the attention is focused on the buckling analysis of glass columns and on the assessment of uncertainties due to input random parameters. With the support of finite element numerical models, a total of 800 glass columns are investigated, by accounting for stochastic variations in the geometry (size and thickness), modulus of elasticity and density of glass, maximum amplitude of the imposed initial imperfection, material type. Based on the Monte Carlo simulation method, the final result takes the form of 2400 simulations, where the post-processing analysis is spent on the derivation of empirical formulations for the correlation of the relevant buckling capacity indicators. From the global out-of-plane bending analysis, the input random parameters are observed to affect severely both long and short columns with different flexural stiffness. Besides, a stable linear correlation is found for some influencing indicators. The attention is thus focused on the sensitivity analysis of critical buckling load, ultimate failure configuration, deflection at collapse, buckling reduction coefficient.

**Keyword:** Glass Columns, Column Buckling, Parametric Analysis, Finite Element (FE) Numerical Models, Monte Carlo Simulation (MCS) Method, Stochastic Modelling

## Introduction

Structural glass elements are notoriously associated to severe susceptibility to possible buckling failure mechanisms. As such, in the last few decades, a multitude of studies have been dedicated to monolithic or laminated glass members with a variable combination of restraints and loading conditions. Various efforts can be found in the literature in the form of experimental, numerical and/or analytical analysis of glass beams in lateral-torsional buckling (Belis *et al.*, 2013; Bedon *et al.*, 2015; Valarinho *et al.*, 2016; Santo *et al.*, 2020), glass members under flexural-torsional buckling (Amadio and Bedon, 2013; Bedon and Amadio, 2014; Huang *et al.*,

2020), plates under in-plane compression and/or shear (Luible and Crisinel, 2005; Bedon and Amadio, 2012), etc.

Regarding the specific topic of column buckling for glass members, (Luible and Crisinel, 2004) first addressed this design issue and tried to develop a general verification approach. In their parametric study, the normalized stability curves for design were calculated with the support of numerical models, for various configurations of technical interest. Further studies and design proposals for monolithic and laminated glass columns have been presented in (Amadio *et al.*, 2011; Bedon and Amadio, 2015). Extensive buckling experiments on various glass columns-both monolithic and laminated-are discussed in (Foraboschi, 2009; Pešek *et al.*,

2016; Liu *et al.*, 2017). Glass columns with more geometrical complexity are also investigated in the literature, including also T- or X-shaped columns (Aiello *et al.*, 2011) hollow-box columns (Kalamar *et al.*, 2016), tubular columns (Kamarudin *et al.*, 2018) or bundled columns (Oikonomopoulou *et al.*, 2017). A recent alternative formulation for the equivalent thickness of laminated glass members in compression has been presented in (D'Ambrosio and Galuppi, 2020).

In most of the cited studies, the buckling analysis of glass members is carried out with the support of experimental tests, non-linear analytical models and additional Finite Element (FE) numerical models that could facilitate a more detailed interpretation of test results, as well as a wider extension of the examined configurations. In most of the cases, however, these calculations are carried out on the base of nominal input parameters, such as material properties, dimensions, etc. In this regard, a more detailed analysis has been carried out with a focus on the actual thickness of glass, given that even small variations can be responsible of severe stiffness and slenderness modifications, thus susceptibility to premature buckling collapse mechanism.

Lubile and Crisinel (2004), for example, considered for their parametric calculation a thickness equal to the 97.61% part of the nominal glass thickness (thus corresponding to the 5% percentile of the normal distribution obtained from their previous experimental thickness measurements). This is also in line with (Kalamar *et al.*, 2016), where several thickness measurements are presented with the support of a laser scanning system.

Besides, the actual role of uncertainties due to random input parameters for the buckling performance of glass members still lacks for general applications and considerations. Literature studies dedicated to the compression buckling of various constructional elements and based on the stochastic analysis, are mostly related to specific issues and conventional materials for constructions, like the buckling performance of cylindrical shells with variable imperfections (Chryssanthopoulos and Poggi, 1995), or laminated composite plates with cutout (Onkar *et al.*, 2007) and others.

As known, the Monte Carlo Simulation (MCS) approach represents an alternative and efficient technique to the stochastic analysis method and has been successfully taken into account for the compressive buckling analysis of various constructional systems. Literature examples can be found for lattice columns with stochastic imperfections (Miller and Hedgepeth, 1979), steel columns (Strating and Vos, 1973; Gonzalez Estrada *et al.*, 2018), thin-walled steel I-

section beams/columns with random imperfections (Schillinger *et al.*, 2010), steel stiffened panels for oil tankers (Gaspar *et al.*, 2012) and even cross-laminated timber panels (Oh *et al.*, 2015). Le *et al.* (2019) predicted the critical buckling load of steel columns, based on hybrid Artificial Intelligence (AI) approaches and AI-derived models, whose robustness was verified with the MCS method.

Also (Ly *et al.*, 2019), in this regard, quantified the effect of random material properties on the critical buckling load of circular columns made of steel. Their parametric study, supported by FE models, included up to 500 numerical simulations. In their paper, it is correctly observed that several models are available in the literature for the buckling analysis of columns under axial compression. However, most of them are deterministic and presume that material uncertainty has no effect on the expected critical buckling load of a given member in compression.

The above concepts can be extended also to glass members in general, where the typically small thickness of relatively flexible and slender elements is a first influencing parameter that enforces their typically high susceptibility to possible buckling phenomena. Besides, many other input parameters should be taken into account.

## Existing Design Method for Glass Columns

Buckling failure and loss of stability represent, as known, a frequent condition of premature collapse for structural glass elements, due to the typical high slenderness of these innovative load-carrying structural elements.

The number of studies and research activities dedicated to stability and typical buckling behaviour of glass columns, beams, panels under various boundary and loading conditions confirms the large interest in this topic and the current lack of knowledge on it. Although a substantial amount of experimental research, development of analytical models and sophisticated numerical simulations has been carried out in the past years, further studies are required.

The buckling behaviour of structural glass elements, especially in the case of laminated glass cross-sections composed of two (or more) glass sheets interacting together by means of thermoplastic films able to transfer shear loads between them-depending on the connection stiffness-is in fact not easy predictable, due to a series of mechanical and geometrical aspects to assess and quantify, see (Blaauwendraad, 2007) and many other analytical, numerical or experimental studies, as also recalled above.

Let's assume, as a reference, the monolithic glass member in Fig. 1. The cross-section has  $B \times t$  dimensions and the column spans over  $L$ . Glass material has a linear elastic behaviour, with  $E = 70$  GPa the Modulus of Elasticity (MoE) and  $\nu = 0.23$  the Poisson's ratio. The member is affected by an initial, sine-shaped global imperfection with maximum amplitude  $u_0$ . Under pure tensile considerations, the nominal cross-section is able to offer a total characteristic strength that is equal to:

$$N_R = Af_{g;k} \quad (1)$$

with,  $f_{g;k}$  the characteristic tensile bending resistance for the glass type in use. The reference nominal values are listed in Table 1 for Annealed (AN), or prestressed Heat-Strengthened (HS) and Fully Tempered (FT) types.

The compressive strength of glass, on the other side, is generally many times higher than the tensile value (approximately 400-600 MPa, (Fink, 2000) and thus results in a common buckling failure that is mostly governed by tensile stress peaks (Luible and Crisinel, 2004; Amadio *et al.*, 2011).

Based on Table 1, the major design issue for glass can be thus expected in the well-known, high natural variability of prestress and strength parameters for such a vulnerable constructional material. Several studies of literature (Nurhuda *et al.*, 2010; Lamela *et al.*, 2014; Veer *et al.*, 2018; Pisano and Carfagni, 2017; Mognato *et al.*, 2017; Kinsella *et al.*, 2018) have been dedicated to the measurement and assessment of these nondeterministic and size-dependent material parameters, hence resulting in specific recommendations and limitation for structural design.

In terms of column buckling design, the effect of different of variable tensile bending strength values for glass on the actual load bearing capacity has been for example analyzed in (Luible and Crisinel, 2004; Amadio *et al.*, 2011), for a selection of configurations. The final effect of any natural surface strength variability manifests in a premature breakage of glass. The issue can be addressed with standardized calculation tools and safety coefficients derived from the experimental material characterization.

According to (Bedon and Amadio, 2015) and Fig. 1, a standardized buckling design approach can take the form of an empirical approach that relates the geometrical and mechanical features of a general glass column to verify to the expected design buckling resistance. Such an approach is inspired by conventional design methods that are in use load bearing columns composed of traditional constructional materials. This is also the case of the Italian technical guideline CNR-DT 210/2013 in support of design of glass structures, where it assumed that the buckling verification is satisfied when:

$$N_{Ed} \leq N_{b,Rd} \quad (2)$$

and the design compressive load  $N_{Ed}$  must be assessed towards the design buckling resistance of the column. This resistance is usually affected by a multitude of mechanical and geometrical parameters and can be calculated as:

$$N_{b,Rd} = \chi Af_{g;d} \quad (3)$$

with  $A = B \times t$  and  $f_{g;d}$  the design tensile bending resistance for the glass type in use (CNR-DT 210/2013, 2013). A key role in Equation (3) and in the overall buckling design approach is then assigned to the well-known buckling reduction factor  $\chi$ , where:

$$\chi = \frac{1}{\Phi + \sqrt{\Phi^2 - \lambda^2}} \quad (4)$$

and:

$$\Phi = 0.5 \left[ 1 + \alpha_{imp} (\lambda - \alpha_o) + \lambda^2 \right] \quad (5)$$

where the imperfection coefficients  $\alpha_o = 0.6$  and  $\alpha_{imp} = 0.71$  have been calibrated on the base of extended parametric numerical analyses and (where possible) literature experimental results. The susceptibility to possible column buckling failure mechanisms increases as far as the normalized slenderness increases:

$$\lambda = \sqrt{\frac{Af_{g;k;st}}{N_{cr}^E}} \quad (6)$$

where,  $f_{g;k;st}$  is the proposed characteristic glass strength for buckling (CNR-DT 210/2013, 2013). Worth to be noted that the highest is the tensile bending strength of glass (thus the expected buckling capacity) and the highest is the slenderness in Equation (6), thus the susceptibility to premature failure (with a low  $\chi$  factor from Equation 4).

Moreover, the Euler's critical buckling load:

$$N_{cr}^E = \frac{\pi^2 EI_y}{L^2} \quad (7)$$

With:

$$I_y = \frac{Bt^3}{12} \quad (8)$$

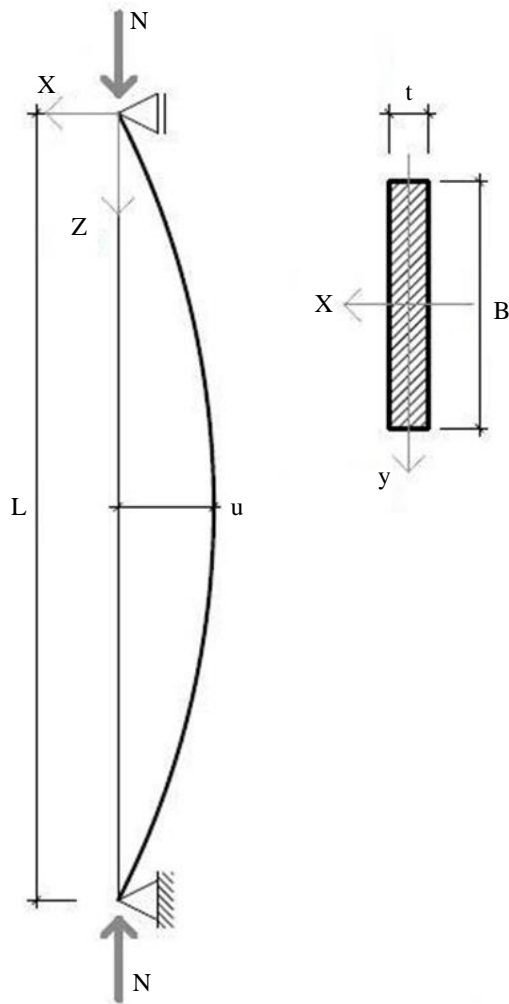


**Fig. 1:** Reference glass column with monolithic  $B \times t$  resisting section and span  $L$  (pinned ends)

**Table 1:** Nominal characteristic values for the tensile bending strength of glass (CNR-DT 210/2013, 2013)

	Glass type		
	AN	HS	FT
$f_{g;k}$ (MPa)	45	70	120

Notoriously represents partial information only for buckling design considerations. On the other side, Equation (7) is one of the first design parameters that are required in the overall calculation process.

The above design formulation represents an efficient generalized approach for monolithic glass members that have been adapted to laminated glass sections (Bedon and Amadio, 2015) and later to glass members and plates under variable loading/boundary conditions, with the used o equivalent thickness formulations. In doing so, the failure tensile resistance of glass for buckling,  $f_{g;k;st}$ , has been set to the characteristic tensile bending value

$f_{g;k}$  (Table 1), thus accounting for various glass types and disregarding any kind of possible residual capacity after the first tensile crack detection.

Within such a standardized approach, it is reasonably expected that many influencing parameters (but especially the actual tensile strength of glass) could affect the overall buckling performance and thus the corresponding input parameters for safe design. On the other side, the same approach allows to account for a single formulation for various glass types and shapes and it is hence efficient for design. The research study from (Feldmann and Langosch, 2010), in this regard, includes a set of buckling experiments on glass elements under in-plane compression and the derivation of a partial safety factor for buckling that has been calculated by taking into account the 75% confidence probability and the 5% fractile for the characteristic value (0.1% fractile for design value) (EN, 1990:2002) (Annex D). Separate safety factor coefficients have been then recommended for HS or FT glass members in compression.

Disregarding the material type (and thus the possible variability in the actual prestress and strength), many other combinations of influencing parameters could lead to premature buckling failure. In the experimental analysis carried out by (Belis *et al.*, 2011), both the shape and size of the initial curvature has been measured for various glass beam specimens (312 in total), proving that a sinusoidal shape can properly describe the initial curvature of beam-like glass elements. The characteristic value of initial imperfection, to account for design calculations, has been thus recommended in mid-span amplitude of  $L/400$ . The same imperfection amplitude is taken into account for the design approach proposed in the CNR-DT 210/2013 document.

## Research Methods

This research study, compared to past literature efforts, focuses on the analysis of the effects on the buckling performance of glass members in compression due to random input parameters. Based on Fig. 1 and the above mathematical model for the standardized buckling verification, major numerical efforts are spent on the side of the member stiffness and susceptibility to possible premature collapse mechanisms. Accordingly, the parametric analysis is carried out on a set of glass columns in agreement with Fig. 1, but inclusive of variable geometry (thickness and span), MoE ( $E$ ), glass type (AN, HS, FT) and global imperfection for the initial sine-shaped bow ( $u_0$ ). Material density  $\rho$  is also included in the set of random parameters, to assess the potential effects on slender members.

In doing so, the Monte Carlo Simulation (MCS) method is used as efficient technique for probabilistic

analysis. MCS is a computational algorithm that relies on repeated random sampling to address risk and uncertainties associated with random input parameters for quantitative analyses and decision making. Also, MCS is one of the simplest and relatively most accurate methods which provides a feasible way to determine the probability of failure, where the limit state function is more complicated (i.e., FE modelling), as also discussed in (Naess *et al.*, 2009; Hadianfard *et al.*, 2018; Johari and Momeni, 2015; Johari *et al.*, 2015) and many other literature studies.

All the reference input properties are hence summarized in Table 2, while Table 3 describes the basic parameters for the MCS (based on truncated normal Probability Density Function (PDF)). The basic material properties are taken from CNR-DT 210/2013. From Table 3, the interval for each parameter is defined as:

$$\begin{aligned} Interval &= [Min, Max] \\ &= [Mean - 3 \times Std, Mean + 3 \times Std] \end{aligned} \quad (9)$$

where, Std is the standard deviation given by:

$$Std = \frac{0.1Mean}{3} \quad (10)$$

According to Fig. 2, through the post-processing analysis of parametric results, the attention is focused on the effects of input parameters on:

- Global load-bearing performance
- Critical buckling load  $N_{cr}^E$
- Failure load  $N_u$
- Buckling reduction coefficient  $\chi$
- Slenderness  $\lambda$
- Failure configuration (failure load  $N_u$  and maximum deflection  $u_{max}$ ) and empirical models are derived in support of design

## Numerical Investigation

### Solving Approach

The FE numerical analysis is carried out in the LS-DYNA computer software, on a wide set of geometrical properties, so as to cover an appropriate range of slenderness ratios for the examined load-bearing members.

As a reference, the “pinned” support condition in Fig. 1 is taken into account, while linearly increasing the imposed axial compressive loads on each glass column. Non-linear incremental analyses are carried out to assess the compressive response of glass columns. Additionally, a geometrical imperfection with global bow  $u_0$  is taken into account for the analysis of a given member. The load-deflection curves from the monotonic incremental analyses are hence separately collected for each

column, while monitoring the evolution of tensile stress peaks, mid-span displacements and reaction forces for the selected monolithic members in out-of-plane bending.

Based on Tables 2 and 3, a total of 800 FE models is thus analyzed for the study herein presented, using MCS. For each configuration, 50 FE models are modelled and analyzed by considering the uncertainty associated with MoE, imperfection and density. The effect of column thickness and span is then considered through different geometrical configurations. In other words,  $800/50 = 16$  different nominal dimensions are taken into account for the examined glass columns. For each one of them, 50 models are then generated based on the variation of MoE, imperfection and density. Finally, for each one of the 800 glass columns, the effect of material type is included in the form of three different nominal strength values representative of AN, HS and FT glass (Table 1), thus resulting in a total of 2400 FE analyses.

Since the manual generation and handling of such a huge number of FE models and output results in LS-DYNA would be extremely hard and time consuming, a set of LS-PrePost, MATLAB, LS-DYNA and C# coding strategies is used in this research study to manage and combine the key input data necessary for the automatic FE modelling, but also for importing the models into LS-DYNA and thus extracting and post-processing the cloud of required FE results.

### Modelling

For the reference pin-end boundary condition explored in this research paper, the corresponding nodal restraint in each glass column is described as in Fig. 3 (detail example of the top section), where it is possible to see that the out-of-plane displacements are constrained for the middle line of nodes, while the possible rotations and vertical displacements are released ( $\delta x = \delta y = 0$ ,  $\delta z \neq 0$ ,  $\theta x = \theta z = 0$  and  $\theta y \neq 0$ ). Similarly, at the base of each column, all the nodes located on the horizontal centerline of the nominal section are constrained in the three spatial directions and angles, with the exception of the rotation around the y-axis ( $\delta x = \delta y = \delta z = 0$ ,  $\theta x = \theta z = 0$  and  $\theta y \neq 0$ ).

**Table 2:** Reference geometrical properties of the examined pinned columns (16 configurations)

	Width $B$ [mm]	Length $L$ [mm]	Thickness $t$ [mm]
Min.	200	500	5
Max.	200	2000	40
Interval	-	500	$\times 2$

**Table 3:** Stochastic properties of input parameters (normal PDF)

Random variable	Mean value	Std.
Imperfection	$L/400$	$(L/200 - L/400)/3$
Density [kg/mm <sup>3</sup> ]	2.5e-6	8.33e-8
MoE [GPa]	70	2.33

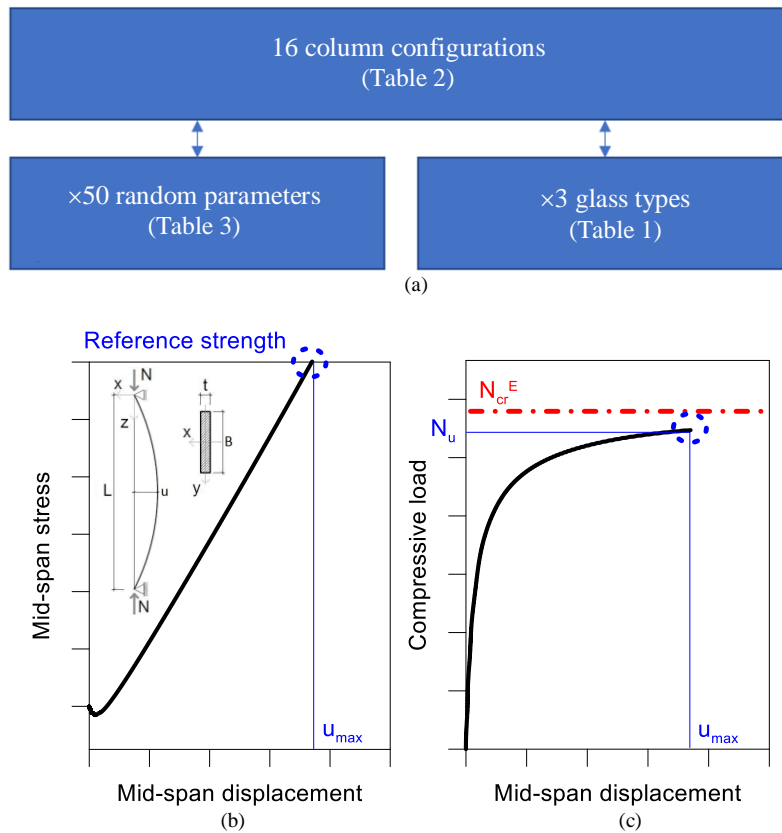


**Fig. 2:** Schematic representation of the (a) numerical procedure and (b)-(c) derivation of selected buckling capacity indicators

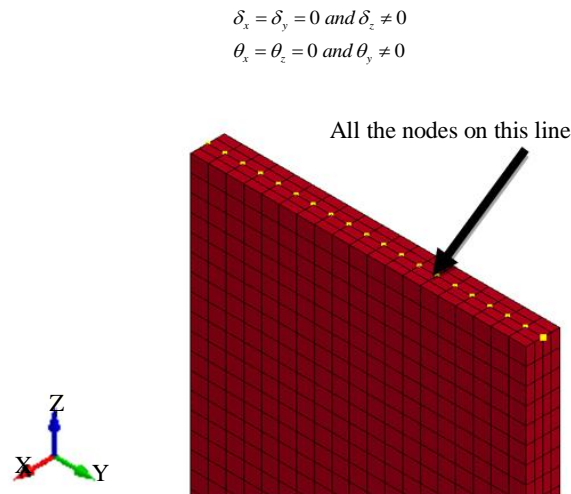


**Fig. 3:** Reference FE model in LS-DYNA (detail of the top restraint)

In the numerical modelling of the selected glass columns, the nominal thickness  $t$  of 5, 10, 20 and 40 mm (Table 2) is divided into  $n_e = 2, 2, 4$  and 6 elements, to ensure a more accurate bending analysis and reliability of results, especially when increasing the thickness value.

Solid elements with dimension  $10 \times 10 \times t_e$  (in mm) are thus used to describe each glass column, where  $t_e$  is the size of the element in the member thickness. Based on the above  $n_e$  values,  $t_e$  is defined in the range from 2.5 to 6.67 mm for nominal thicknesses of 5, 10, 20 and 40 mm respectively.

Regarding the characterization of glass, the MAT\_ELASTIC material model is used for all the FE models, with input properties from Table 3, while the nominal resistance values from Table 1 are indirectly accounted in the post-processing stage.

Each FE model is preliminary subjected to an initial sine-shaped geometrical imperfection as in Table 3. Based on literature efforts, its shape is basically detected in the first fundamental modal shape of a pinned column and thus imported as a reference geometrical configuration. Disregarding the variability of real imperfection shapes (Belis *et al.*, 2011) and thus assuming the worst bending effects to derive from a conventional imperfection shape, the attention is focused on the analysis of bending and buckling effects deriving from the imposed maximum amplitude  $u_0$  of this imperfection that is progressively modified as in Table 3.

Through the typical FE analysis of the so pre-deformed glass columns, finally, the in-plane compressive load  $N$  is imposed to the top section of each model and modified with a ramp function in the time of the simulation, so that it could be gradually increased until any kind of buckling collapse mechanism. To this aim, according to literature, the propagation of tensile stress peaks is continuously monitored as a function of the imposed compressive load  $N$ . The reference analysis is then interrupted at the first achievement of a maximum tensile bending stress in glass at least equal to the assigned material strength (Table 1). The possible occurrence of an overall buckling deformation in the large displacement field can represent an alternative collapse configuration for slender members and it is thus additionally taken into account for the analysis of the collected parametric FE results. In this manner, especially for long span members, it is ensured that the derived resistance value at collapse can be representative of their maximum capacity.

## Discussion of Numerical Results

### Boundaries

The random parameters from Tables 2 and 3 were selected in a preliminary stage of the study, so as to cover a wide range of potential scenarios of technical interest, even in presence of a relatively small number of total simulations. In this regard, Fig. 4 shows the overall examined configurations for the 800 column geometries/mechanical properties, both in terms of MoE distribution (Fig. 4a) and compressive performance, i.e., in the form of the  $N_{cr}^E/N_R$  ratio for all the analyzed members (Fig. 4b). Similarly, Fig. 5

shows the distribution of examined slenderness ratios  $\lambda$  (Equation 6). The random input values, as shown, are grouped by glass type (AN, HS and FT) and typically include very short members ( $\lambda < 3$ ) but also glass columns with a relatively high sensitivity to out-of-plane deformations ( $\lambda > 10$ ).

Finally, in Fig. 6, the variation of the theoretical critical buckling load  $N_{cr}^E$  (Equation 7) is proposed as a function of the measured slenderness ratio  $\lambda$  (Equation 6) for all the examined configurations. Again, the comparative dots are grouped in terms of glass type and confirm the wide distribution of explored scenarios.

### Load-Bearing Performance

The typical load-bearing response of glass columns is investigated in terms of imposed compressive load  $N$  and measured mid-span deflection or tensile stress peak in the glass section. For all the examined glass columns, the failure configuration is numerically detected as the first attainment of a maximum tensile stress in bending at least equal to the nominal resistance of AN, HS or FT glass respectively, thus 45, 70 and 120 MPa (Table 1). In this study, any kind of variability in the material resistance is disregarded (Kinsella *et al.*, 2018), while imposing random mechanical and geometrical parameters to the set of 800 members ( $\times 3$  glass types).

Selected examples are proposed in Figs. 7a and 7b respectively, for a given AN member (with nominal dimensions  $L = \text{var} \times B = 200 \times t = 5$  mm). The first influencing parameter that is expected to affect the overall out-of-plane bending performance is certainly the slenderness of each column (i.e., Equation 6), as also shown in Fig. 7. Besides, the assumption of random input properties for 16 different glass columns is typically observed to result in a multitude of possible configurations and thus in a number of additional influencing parameters that should be separately assessed for each one of the selected columns.

In this regard, some additional examples are proposed in Figs. 8a and 8b, for a given member (with nominal dimensions  $L = 500 \times B = 200 \times t = 5$  mm) composed of AN, HS or FT glass respectively (random input properties agreeing with Tables 2 and 3). The numerical comparative plots of Fig. 8 are interrupted at the first achievement of a maximum tensile bending stress equal to the assigned characteristic strength value. Moving from the AN to the FT column, as shown, the overall bending performance remarkably increases as a direct effect of the resistance increase ( $\approx 2.6$  the nominal strength magnification factor from Table 1). As also expected, moreover, the effect of input

random parameters (especially the MoE value and the imperfection amplitude) can be clearly perceived from the first stage of the load-deflection compressive response, hence resulting in possible severe variations in terms of ultimate compressive load  $N_u$  at collapse.

In Figs. 9 and 10, similar results are presented for the same geometrical system, but assuming that the members in compression are composed of AN or FT glass. In this case, the whole cloud of FE data is proposed for each column ( $\times 50$  model derivations).

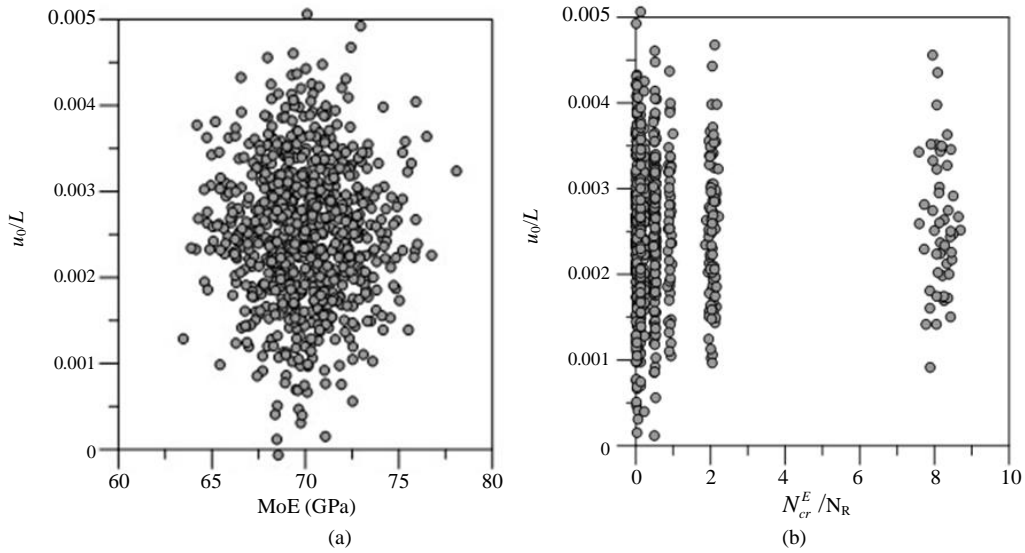


**Fig. 4:** Distribution of the examined (a) MoE values and (b)  $N_{cr}^E/N_R$  ratios, as a function of the amplitude  $u_0/L$  (input parameters from Tables 2 and 3)

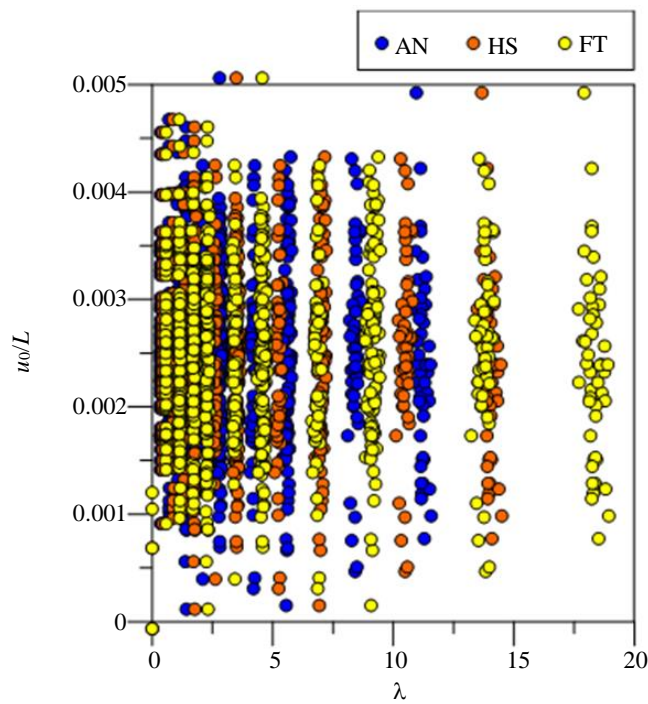


**Fig. 5:** Distribution of the examined slenderness values  $\lambda$  for AN, HS and FT glass columns, as a function of the initial imperfection amplitude  $u_0/L$  (input parameters from Tables 2 and 3)



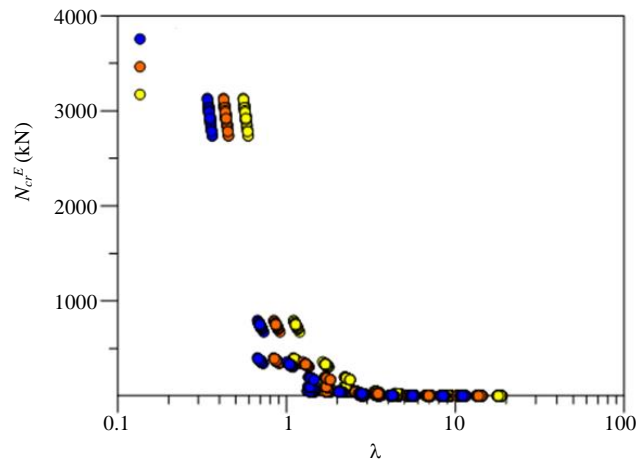
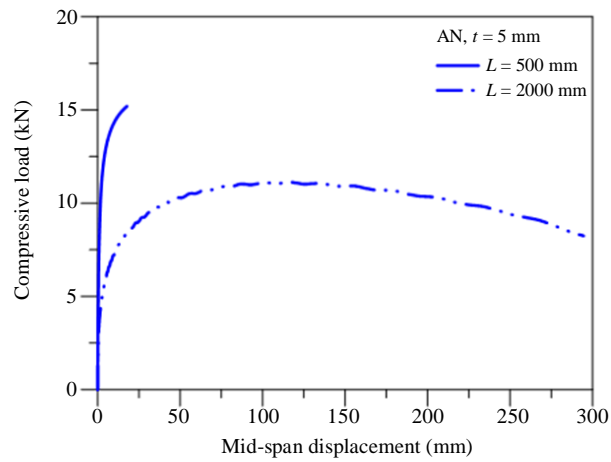
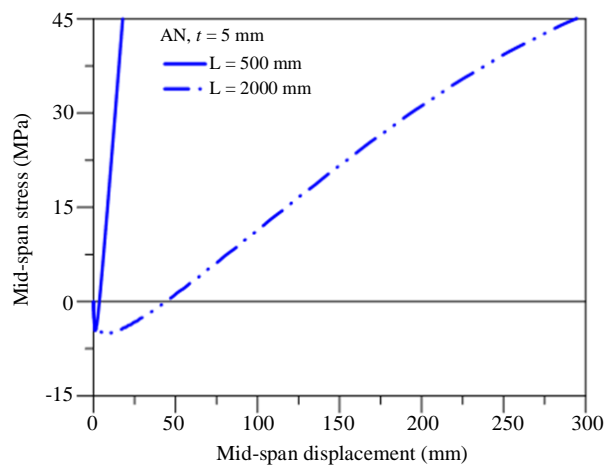


**Fig. 6:** Distribution and variation of the critical buckling load  $N_{cr}^E$  (Equation 7), as a function of the column slenderness  $\lambda$  (Equation 6), for the 800 examined AN, HS or FT glass columns (input parameters from Tables 2 and 3).

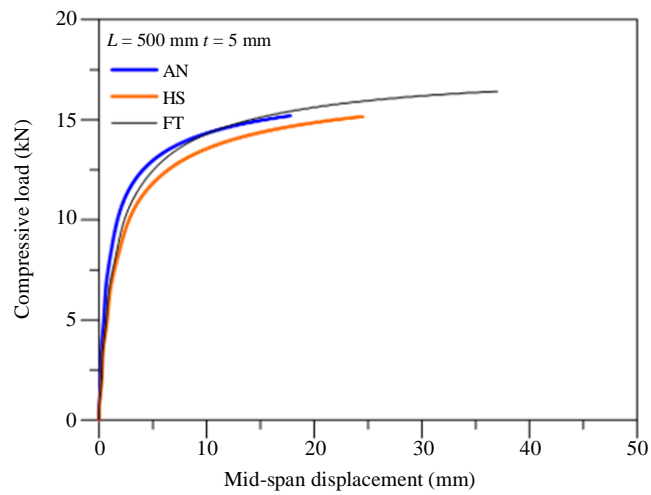


(a)

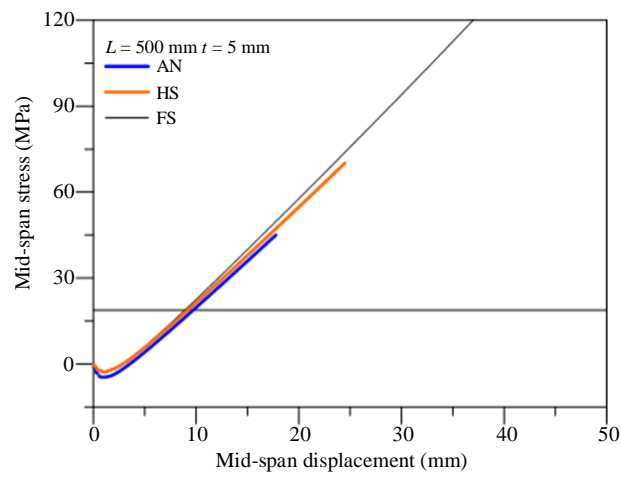


(b)

**Fig. 7:** (a) Load-deflection and (b) load-stress response of two selected AN glass columns (with nominal dimensions  $L = var \times B = 200 \times t = 5$  mm)

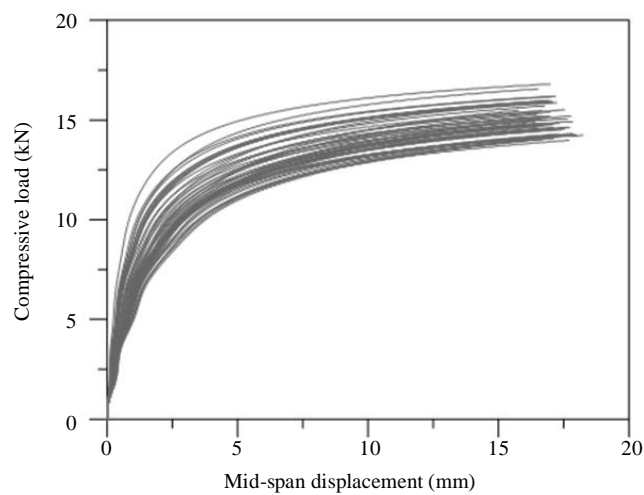


(a)



(b)

**Fig. 8:** (a) Load-deflection and (b) load-stress response of two selected glass columns (with nominal dimensions  $L = 500 \times B = 200 \times t = 5 \text{ mm}$ ) composed of AN, HS or FT glass



(a)

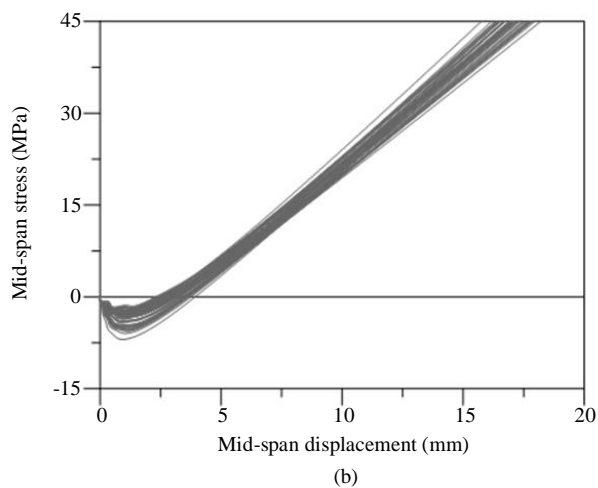


**Fig. 9:** (a) Load-deflection and (b) load-stress response of 50 selected AN glass columns (with nominal dimensions  $L = 500 \times B = 200 \times t = 5$  mm)

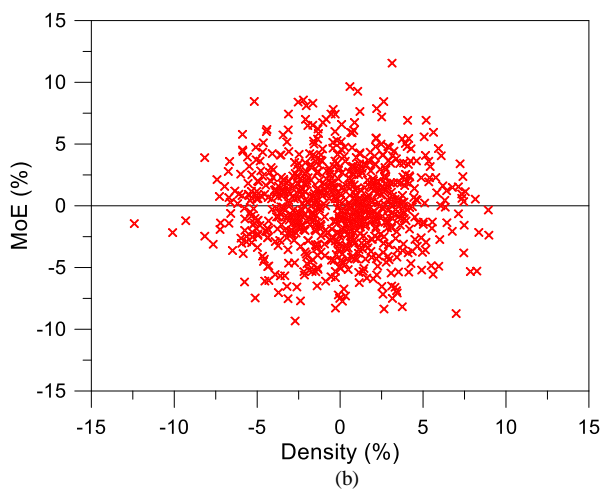
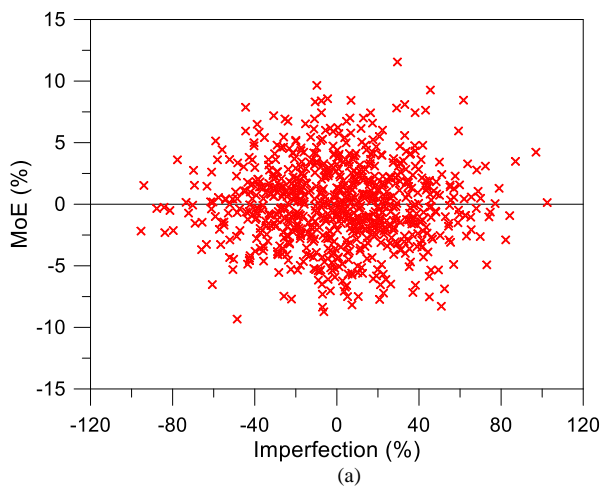


**Fig. 10:** Distribution of MoE, density and imperfection variation (% scatter), compared to input nominal values, for all the examined columns ( $800 \times$  glass type)

While each analysis is still separately interrupted at the first achievement of a tensile stress peak at least equal to the reference material strength in Table 1, it can be perceived that the overall collected FE plots are rather scattered in the initial flexural stiffness, maximum capacity and failure configuration, as a major effect of the stochastic distribution of input data in Tables 2 and 3. More in detail, from the whole parametric study it is also observed that:

- MoE variations directly affect the bending stiffness of the glass members object of analysis and thus their sensitivity to out-of-plane deformations. Due to MoE variations only, the percentage scatter for the calculated flexural stiffness values (and thus critical buckling load  $N_{cr}^E$  of the same member) is found in the range of  $\pm 15\%$  compared to the nominal MoE (Fig. 10)
- The amplitude of the initial global bow,  $u_0$ , is a further well-known, relevant influencing parameter, given that it can manifest in a premature loss of stability for the whole glass member object of study. For the selected random parameters, a relatively high variation is calculated in peak values of  $\pm 80\%$  the nominal ones (Fig. 10a)
- The effects of both MoE and  $u_0$  parameters are strictly connected to the slenderness  $\lambda$  of the examined members. In this research study and specifically for relatively short glass members (expected to collapse for mainly compressive issues, rather than buckling-related phenomena), very high sensitivity can be observed to the assigned input parameters (i.e., Fig. 9), in the same way of long/slender members (i.e., Fig. 11)
- Finally, the possible variation in the material density  $\rho$  could represent a relevant parameter for compressive buckling assessment purposes. Typical input values are shown in Fig. 10b. Compared to the other random parameters, however,  $\rho$  is observed to have minimum effects, that can be slightly perceived for glass columns with high slenderness  $\lambda$

In this regard, the post-processing stage of the collected FE results can be further maximized as far as they are used for the definition of potential empirical models that could capture any kind of correlation.

### Critical and Failure Loads

The critical load  $N_{cr}^E$  for columns represents, as known, a poor parameter only for the assessment of the actual buckling capacity and response of a given member. A multitude of parameters, including geometrical and mechanical aspects, are responsible of the final capacity and thus of the buckling failure,

$N_u$ , for the examined members. Even more sensitivity of their actual capacity can be expected under random input parameters, as also previously observed from Figs. 9 and 11.

To provide a more detailed interpretation of buckling measurements (especially in the case of background experimental measurements), the Southwell plot approach (Southwell, 1932) can be efficiently taken into account. This method assumes that from the experimental (or even numerical) measurements (plotted in the form  $u/N$  versus  $u$ , with  $u$  the maximum out-of-plane displacement due to the increasing applied compressive load  $N$ ), the slope of fitting curves can be rationally determined for the examined load bearing members. The advantage of the approach (as far as the examined load bearing members behave elastically) is the possible minimization (or even avoidance) of cost-consuming and destructive laboratory experiments. Successful applications can be found (for glass/buckling-related applications) in (Belis *et al.*, 2013) and many others. The first indication provided by Southwell plots is in fact the critical load of a member, given by the slope of the linear fitting curve which at best approximates the  $u-(u/N)$  plot of available results. At the same time, the interception between this linear fitting curve and the y-axis gives an indication of the initial lack of straightness of the tested specimens and in particular the maximum amplitude  $u_0$  of possible geometrical imperfections or boundary and load eccentricities.

In this study, given the lack of experimental studies and the final goal of the analysis, the attention is focused on the quantification of uncertainties due to random input parameters for the buckling performance assessment of glass columns. The final results turn out in fact in potential sensitivity of the traditional design parameters and coefficients that are used to support safe design calculations.

The collected results in Fig. 12, for example, are selected to present an overview of random parameters effects on both the critical and failure load of grouped column geometries (with 50 simulations for each nominal geometry  $\times$  glass type, based on Tables 2 and 3). In Fig. 11a, more in detail, the attention is focused on the variation of  $N_{cr}^E$  (Equation 7) with the slenderness  $\lambda$  (Equation 6). The trend of collected values is generally found to be perfectly linear, based on the selected interval of random variables in Tables 2 and 3, as well as on the theoretical basis of the calculated  $N_{cr}^E$  and  $\lambda$  values. The same dots are then grouped by glass type that basically affects the slenderness value only (due to resistance variations in Equation 6).

In Fig. 12b, selected FE results are indeed proposed in terms of ultimate load at failure,  $N_u$ , for groups of AN, HS or FT glass columns with similar nominal geometry and random input parameters from Tables 2 and 3.

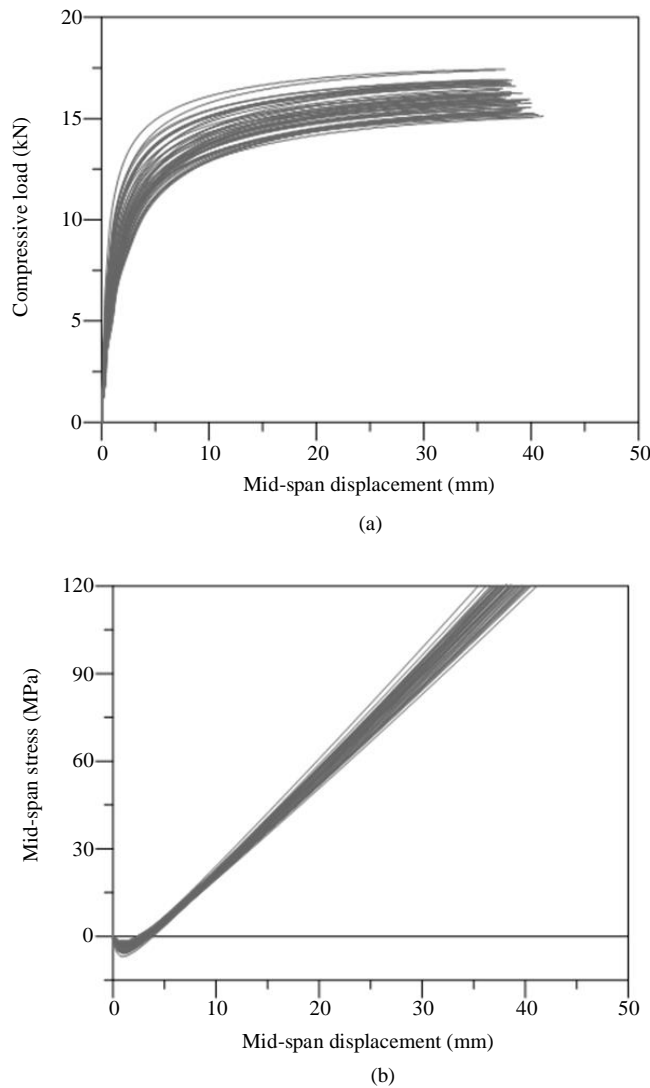
Given that the collected  $N_u$  results strictly depend on the section features and material properties, but also on the amplitude of the imposed geometrical imperfection, from Fig. 12b it is possible to notice that the grouped FE data are still shifted in slenderness  $\lambda$  as a function of the assigned material type (AN, HS or FT). However, a more pronounced scatter can be observed in their linear trend, compared to Fig. 12a, as a direct combination of effects due to the stochastic analysis.

### Linear Regression at Failure

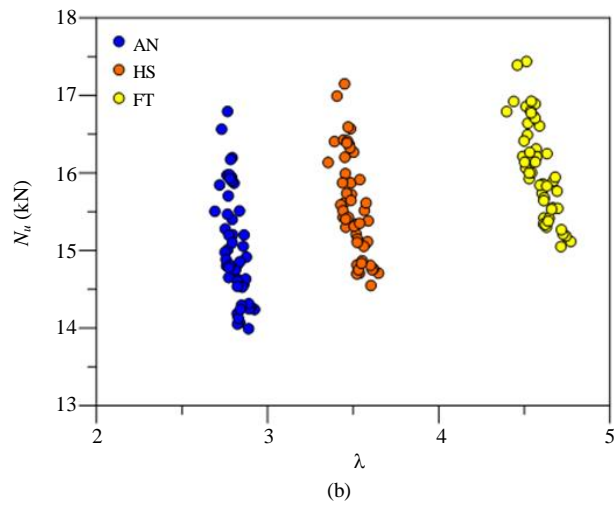
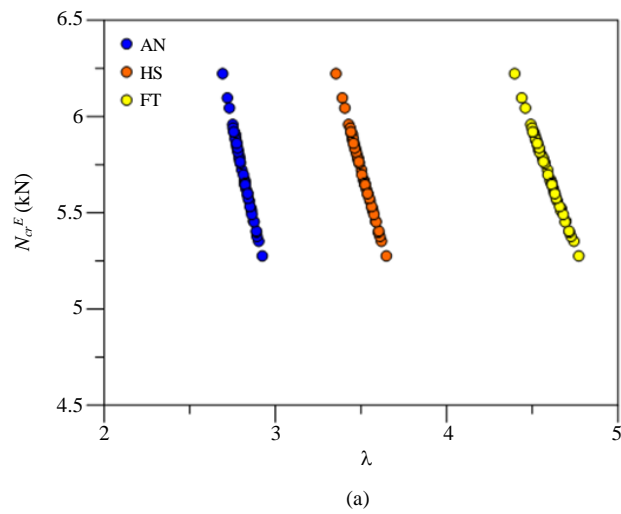
Part of the study is then focused on the analysis of failure condition for the examined columns, as a function of random input parameters. As such, parametric values are discussed in terms of maximum mid-span

deflection ( $u_{max}$ ) and ultimate compressive load  $N_u$ , corresponding to the first achievement of the limit/allowable tensile stress in glass. The repetition of the same approach for all the glass columns can support the definition of a series of charts or empirical models of practical use. Typical examples are shown in Fig. 13 for all the examined 2400 column configurations and thus grouped in Figs. 13a to 13c by glass type (800 members composed of AN, HS or FT glass).

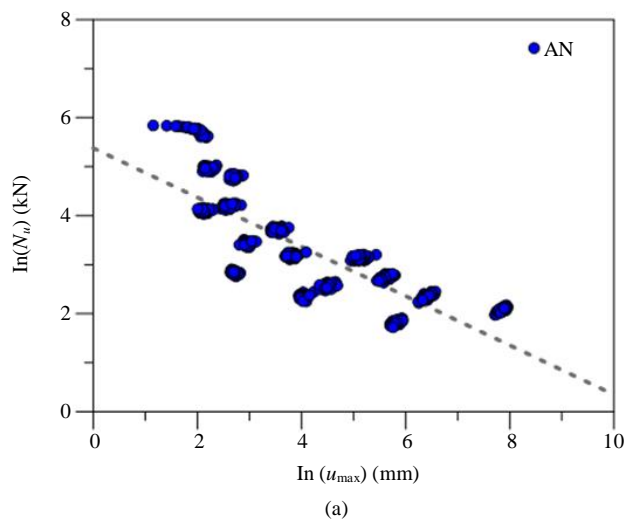
The collected FE data, moreover, are proposed in a bi-logarithmic system, so as to facilitate the analytical correlation of the available data. Worth of interest, in this sense, is the trend of the linear regression curves that are proposed in each graph, in order to capture the mean trend of the corresponding cloud of numerical data.



**Fig. 11:** (a) Load-deflection and (b) load-stress response of 50 selected FT glass columns (with nominal dimensions  $L = 500 \times B = 200 \times t = 5$  mm)



**Fig. 12:** Variation of the (a) critical buckling load  $N_{cr}^E$  (Equation 7) or (b) ultimate failure load  $N_u$ , as a function of the column slenderness  $\lambda$  (Equation 6), for selected AN, HS or FT glass columns (selected examples with similar nominal geometry and grouped



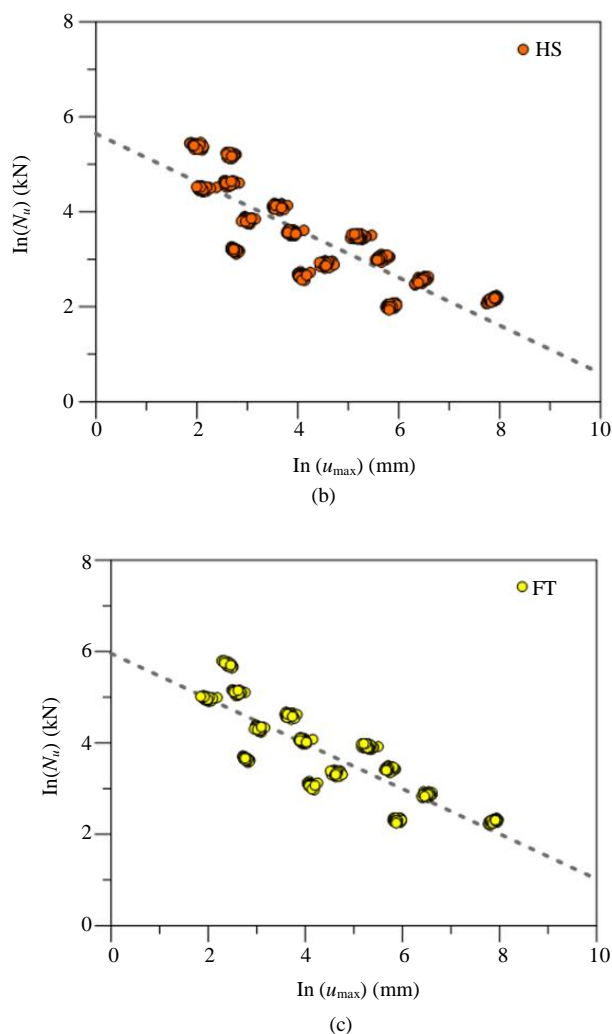


**Fig. 13:** Bi-logarithmic linear regression of ultimate deflection and load for selected glass columns (2400 simulations in total) composed of (a) AN, (b) HS (c) FT glass

Besides the random variation of some key input parameters for the buckling analysis of glass columns, it can be seen a rather constant slope for the three linear regression curves in Fig. 13. At a first analysis, this effect can result from the use of nominal resistance values for different glass types (Table 1), but it also confirms that the glass type itself (with nominal resistance values spanning from 45 to 120 MPa) does not largely affect the overall trend of predicted failure configurations.

This is also the case of the practical other input random parameters that are derived from Tables 2 and 3. The linear regression curves for the comparative FE data in Fig. 13 shows in fact a progressive increase of the constant parameter (i.e., intercept value of the regression curve with the y-axis) for different glass types. This value is calculated in the order of 5.38 kN for AN members, 5.64 kN for HS and 5.96 kN for FT members.

Again, the correlation of these values with the nominal resistance of the examined glass types (Table 1) shows that:

- A mostly linear and stable variation can be observed in terms of failure configuration for the examined glass members, in terms of regression curves (slope and y-axis intercept) and glass type (nominal tensile strength of AN, HS or FT glass). This outcome is further emphasized in Fig. 14

Besides, when the same comparative results are discussed towards the weakest AN glass type, it is observed that:

- For HS glass columns (+55.5% theoretical increase of tensile resistance, compared to AN glass), their actual buckling capacity at failure can increase in the order of +4.9%

- In the case of FT glass members (+166.6% of tensile resistance, compared to AN glass), the capacity at failure is expected to increase (for a glass member with similar input parameters) in the order of +10.9%

### Buckling Reduction Coefficient

In Fig. 15, a selection of FE data is proposed for one of the examined geometries (nominal dimensions  $L = 500 \times B = 200 \times t = 5$  mm), by changing the material type (50 simulations  $\times$  glass type). The failure configuration is first detected as in Fig. 2. Moreover, the Euler's critical load  $N_{cr}^E$  is calculated from Equation (7), based on the actual input mechanical properties for each one of the examined columns. Finally, the buckling reduction coefficient  $\chi$  is numerically derived as:

$$\chi = \frac{N_u}{N_R} \quad (11)$$

where,  $N_R$  is given in Equation (1).

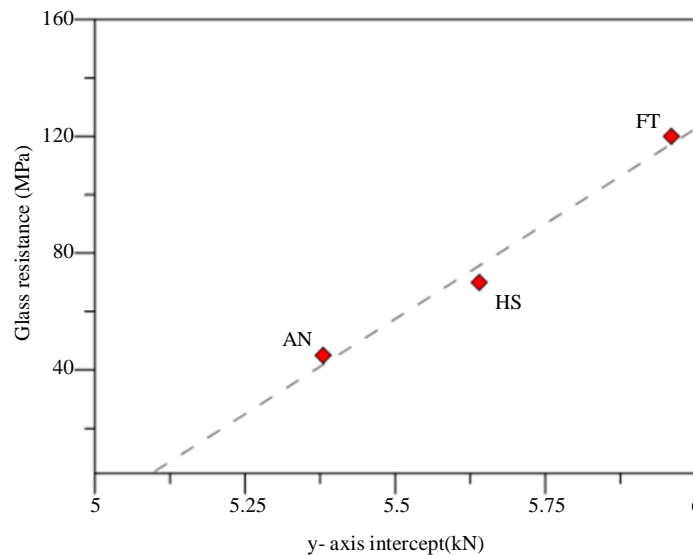
The final result of the FE study takes the form of the conventional standardized approach for design buckling curves, in which the input geometry of the column to verify is expressed in terms of normalized slenderness  $\lambda$  (Equation 6) and the actual buckling capacity takes the form of the well-known buckling reduction coefficient  $\chi$  (as obtained, in this study, from a number of  $800 \times 3$  FE analyses and Equation 11). In Fig. 16, the sensitivity of

the so collected data are proposed for a group of glass columns, divided by glass type/strength.

### Maximum Mid-Span Displacement

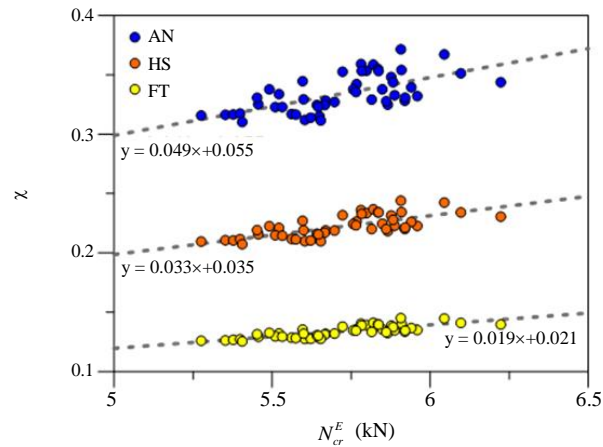
In conclusion, a further attempt of interpretation of parametric relevant FE data are derived from the MCS analysis of the available results. Figures 17-19, in this regard, show the PDF of the maximum mid-span displacement of AN, HS and FT glass columns ( $u_{max}$ ) with nominal dimensions  $L = 500 \times B = 200 \times t = 5$  mm, as obtained by MCS with 50 simulations. In the figures, the PDFs are not smooth curves due to the fact that an higher number of simulations should be selected. Based on past literature efforts, an acceptable strategy for determining the PDF is to carry out reasonable number of simulations and fit a suitable PDF to the computed distribution which can hence be used for calculating the probability of failure and other relevant parameters, like the reliability index. In this study, a normal PDF is thus fitted in order to obtain a smooth distribution in each investigated case.

Figure 19, moreover, shows the PDF of maximum mid-span displacement for AN, HS and FT glass columns. From these figures, the mean of maximum mid-span displacement for AN, HS and FT glass columns are calculated in 17.062 mm ( $\approx L/30$ ), 24.328 mm ( $\approx L/20$ , +42.58%) and 38.388 mm ( $\approx L/13$ , +124.99%), respectively. A linear trend agreeing with Fig. 14 can be confirmed also in this case. Similarly, from Fig. 19, the Std values of the measured mid-span displacement for AN, HS and FT glass columns are calculated in 0.509, 0.571 and 1.449 mm, respectively.



**Fig. 14:** Linear trend of regression-based y-axis intercept values (from Fig. 13) as a function of the characteristic resistance of AN, HS or FT glass types, as obtained at buckling failure from the analysis of 2400 columns ( $800 \times 3$  glass type simulations)





**Fig. 15:** Numerically calculated buckling reduction factor  $\chi$ , as a function of the critical buckling load  $N_{cr}^E$ , as obtained for AN, HS or FT glass columns (50 simulations/glass type, with nominal dimensions  $L = 500 \times B = 200 \times t = 5\text{mm}$ )

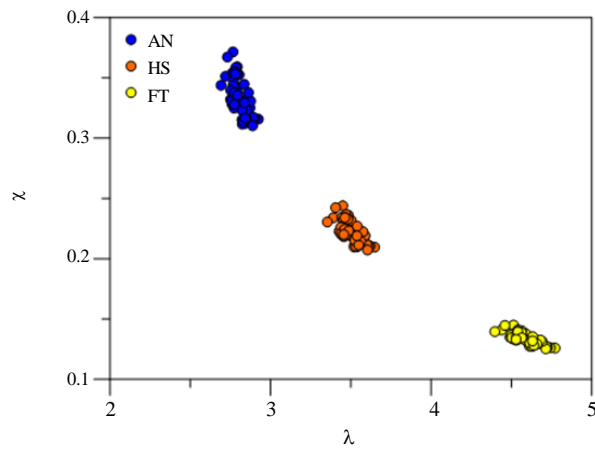


**Fig. 16:** Numerically calculated buckling reduction factor  $\chi$ , as a function of the normalized slenderness  $\lambda$ , as obtained for AN, HS or FT glass columns (50 simulations  $\times$  glass type, with nominal dimensions  $L = 500 \times B = 200 \times t = 5\text{ mm}$ )

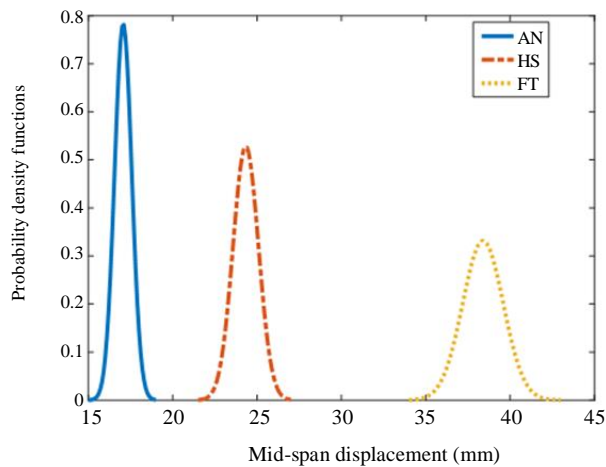


**Fig. 17:** Probability density functions of the mid-span displacement of AN, HS and FT glass columns (50 simulations  $\times$  glass type, with nominal dimension  $L = 500 \times B = 200 \times t = 5\text{ mm}$ )

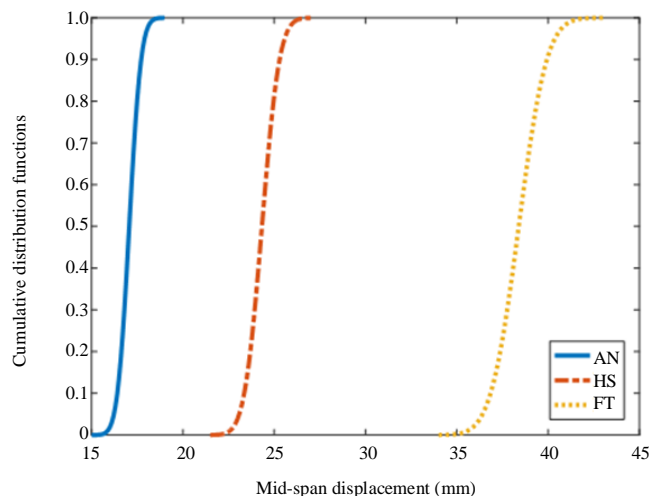
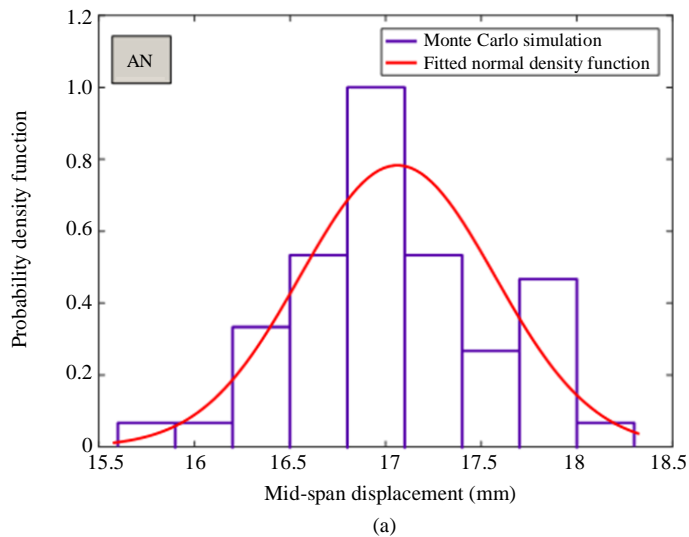
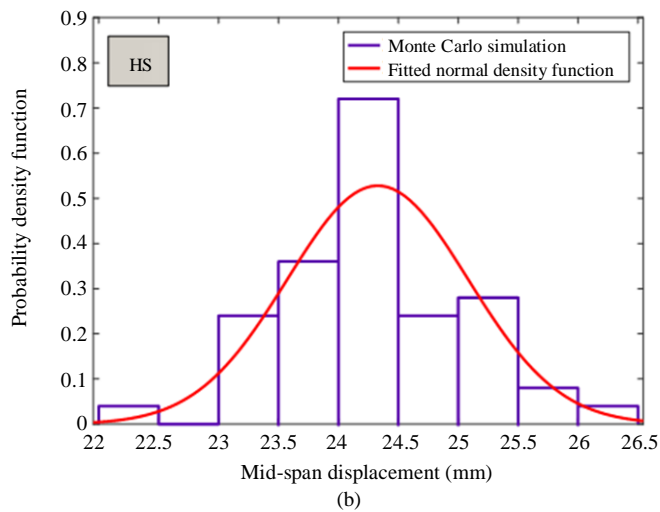


**Fig. 18:** Cumulative distribution functions of the mid-span displacement of AN, HS and FT glass columns (50 simulations  $\times$  glass type, with nominal dimension  $L = 500 \times B = 200 \times t = 5$  mm)



(a)



(b)

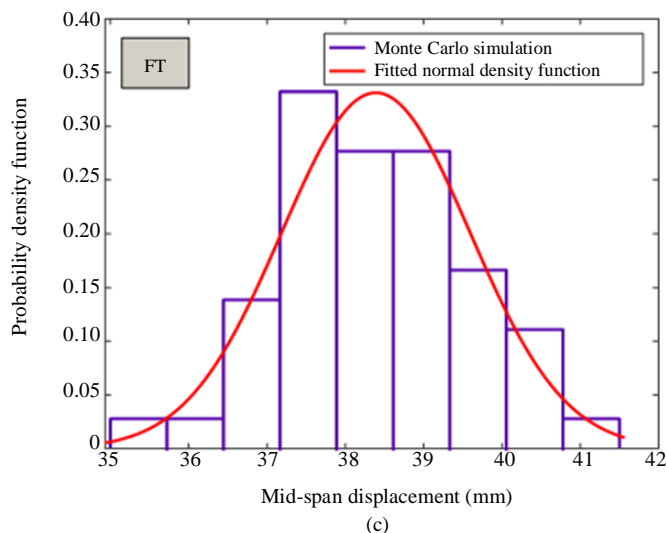


**Fig. 19:** MCS results and fitted normal density function for the mid-span displacement of (a) AN, (b) HS or (c) FT glass columns at failure (50 simulations/glass type, with nominal dimension  $L = 500 \times B = 200 \times t = 5$  mm)

This last result in terms of Std shows that the value increases as the column composition (even with similar elastic and geometrical features) moves from AN to FT material properties. The largest variation (or Std) belongs in fact to FT glass columns with higher tensile resistance, which means that the fluctuation of input parameters has a more remarkable effect on their overall buckling performance and resistance. Looking back at Equation (6), the FT glass type for a given member corresponds to higher slenderness value, thus limited buckling capacity (and lower  $\chi$  factor in Equation 4) that derives from the high flexibility and sensitivity to input random parameters.

As a nutshell, the effect of uncertainties increases as the glass column composition changes from AN to FT and the behaviour of FT glass columns is more sensitive to uncertainties, respect to the other glass types.

## Conclusion

Structural glass elements that are used for engineering applications typically require specific design and verification methods that are required to ensure appropriate safety levels. Among others, the buckling verification of these members is a crucial step, given that they are commonly characterized by high slenderness ratios and can be thus highly susceptible to premature collapse mechanisms due to stability losses. As such, several studies are available in the literature, in support of the development or refinement of suitable design approaches. Background documents can be found for glass columns, beams, plates under ideal or non-ideal loading and boundary conditions.

Generally, it is recognized that the use of experimental methods should be sufficiently extended to cover a number of possible uncertainties and variabilities in the key input parameters, so as to support a reliable

calibration of design recommendations and rules. In this regard, the finite element numerical approach can offer a robust support and minimize the experimental efforts. At the same time, the natural remarked variability of glass strength is expected to represent the first influencing parameter for design.

In this study, the attention was thus focused on the analysis of the buckling performance of glass column. Differing from past literature effort, specific attention was given to the analysis of uncertainties due to input random parameters for the buckling capacity of glass members. Based on efficient Finite Element numerical models, a total of 2400 glass columns (800 mechanical and geometrical configurations  $\times$  three glass types) were investigated, by accounting for stochastic variations in the geometry, size, thickness, but also modulus of elasticity of glass and maximum amplitude of the imposed initial imperfection, as well as glass type/resistance. Empirical formulations were presented in support of the collected numerical results, by taking advantage of the Monte Carlo simulation approach.

From the discussed parametric studies, it was proved that:

- In terms of global buckling performance, the use of input random parameters (geometrical and material properties) has comparable effects on slender or short columns
- The use of a linear regression method for buckling correlations suggested a stable evolution of the failure configuration for all the examined columns, even with random input parameters and different glass types/nominal strength values
- The classical calculation approach for the buckling reduction coefficient  $\chi$  showed a rather

stable linear trend with the theoretical critical load  $N_{cr}^E$ . Major sensitivity to random parameters was observed for AN glass, with a progressive decrease for HS and FT glass columns

- For the given set of glass columns, the use of AN glass or prestressed HS (+55.5% strength) and FT (+166.6% strength) glass types was quantified in a theoretical increase of  $\approx 5\%$  (HS) and  $\approx 10\%$  (FT) buckling capacity (based on stress peaks control). Such a buckling capacity tendency towards the glass type is expected to further minimize as far as the actual material resistance has some variations from the nominal values
- Similarly, the analysis of comparative FE results in terms of ultimate mid-span deflection at failure proved that the sensitivity of buckling capacity estimates to random parameters increases as far as the glass strength of glass increases (thus is minimum for AN columns). The typical high flexibility of these members is hence responsible of major sensitivity effects that prevail on the improved resistance capacity of prestressed glass types
- It is finally worth to be noted that the whole parametric study has been carried out under the assumption of ideal restraints for the examined glass columns. Additional sensitivity is thus expected in presence of partial local flexibility due to soft materials that are typical of glass applications

### Author's Contributions

**Mohammad Momeni:** Numerical modelling, parametric analysis, discussion of results, paper drafting, review.

**Chiara Bedon:** Supervision, discussion of results, paper drafting, review.

### Ethics

This article is original and contains unpublished material. The corresponding author confirms that all of the other authors have read and approved the manuscript and no ethical issues involved.

### References

Aiello, S., Campione, G., Minafò, G., & Scibilia, N. (2011). Compressive behaviour of laminated structural glass members. *Engineering Structures*, 33(12), 3402-3408.

Amadio, C. L. A. U. D. I. O., & Bedon, C. H. I. A. R. A. (2011). Buckling of laminated glass elements in compression. *Journal of structural Engineering*, 137(8), 803-810.

Amadio, C., & Bedon, C. (2013). A buckling verification approach for monolithic and laminated glass elements under combined in-plane compression and bending. *Engineering structures*, 52, 220-229.

Bedon, C., & Amadio, C. (2012). Buckling of flat laminated glass panels under in-plane compression or shear. *Engineering Structures*, 36, 185-197.

Bedon, C., & Amadio, C. (2014). Flexural-torsional buckling: experimental analysis of laminated glass elements. *Engineering structures*, 73, 85-99.

Bedon, C., & Amadio, C. (2015). Design buckling curves for glass columns and beams. *Proceedings of the Institution of Civil Engineers-Structures and Buildings*, 168(7), 514-526.

Bedon, C., Belis, J., & Amadio, C. (2015). Structural assessment and lateral-torsional buckling design of glass beams restrained by continuous sealant joints. *Engineering Structures*, 102, 214-229.

Belis, J., Bedon, C., Louter, C., Amadio, C., & Van Impe, R. (2013). Experimental and analytical assessment of lateral torsional buckling of laminated glass beams. *Engineering Structures*, 51, 295-305.

Belis, J., Mocibob, D., Luible, A., & Vandebroek, M. (2011). On the size and shape of initial out-of-plane curvatures in structural glass components. *Construction and Building Materials*, 25(5), 2700-2712.

Blaauwendraad, J. (2007). Buckling of laminated glass columns. *Heron-English Edition*, 52(1/2), 147.

Chryssanthopoulos, M. K., & Poggi, C. (1995). Stochastic imperfection modelling in shell buckling studies. *Thin-walled structures*, 23(1-4), 179-200.

CNR-DT 210/2013. (2013). Istruzioni per la progettazione, l'esecuzione ed il controllo di costruzioni con elementi strutturali di vetro, National Research Council, Rome, Italy, Technical Document (in Italian)

D'Ambrosio, G., & Galuppi, L. (2020). Enhanced effective thickness model for buckling of LG beams with different boundary conditions. *Glass Structures & Engineering*, 1-6.

EN. (1990:2002) Eurocode - Basis of structural design. CEN, Brussels, Belgium.

Feldmann, M., & Langosch, K. (2010). Buckling resistance and buckling curves of pane-like glass columns with monolithic sections of heat strengthened and tempered glass. In *Challenging Glass Conference Proceedings (Vol. 2, pp. 319-330)*.

Fink, A. (2000). Ein Beitrag zum Einsatz von Floatglas als dauerhaft tragender Konstruktionswerkstoff im Bauwesen. *Inst. für Statik*.

Foraboschi, P. (2009). Buckling of a laminated glass column under test. *Struct Eng*, 87(1), 2-8.

Gaspar, B., Naess, A., Leira, B. J., & Soares, C. G. (2012). System reliability analysis of a stiffened panel under combined uniaxial compression and lateral pressure loads. *Structural safety*, 39, 30-43.

- Gonzalez Estrada, O. A., Martinez, J., & Casanova, E. (2018). Sensitivity analysis of a member under compression via Monte Carlo method. *Revista Uis Ingenierías*.
- Hadianfard, M. A., Malekpour, S., & Momeni, M. (2018). Reliability analysis of H-section steel columns under blast loading. *Structural Safety*, 75, 45-56.
- Huang, X., Cui, M., Liu, Q., & Nie, J. (2020). An experimental study on the structural behaviour of laminated glass members under combined axial compression and in-plane bending. *Materials and Structures*, 53, 1-14.
- Johari, A., & Momeni, M. (2015). Stochastic analysis of ground response using non-recursive algorithm. *Soil Dynamics and Earthquake Engineering*, 69, 57-82.
- Johari, A., Momeni, M., & Javadi, A. A. (2015). An analytical solution for reliability assessment of pseudo-static stability of rock slopes using jointly distributed random variables method.
- Kalamar, R., Bedon, C., & Eliášová, M. (2016). Experimental investigation for the structural performance assessment of square hollow glass columns. *Engineering Structures*, 113, 1-15.
- Kamarudin, M. K., Yusoff, M. M., Disney, P., & Parke, G. A. (2018, August). Experimental and numerical investigation of the buckling performance of tubular glass columns under compression. In *Structures* (Vol. 15, pp. 355-369). Elsevier.
- Kinsella, D., Lindström, J., & Persson, K. (2018). Performance of standard statistical distributions for modelling glass fracture. *International journal of structural glass and advanced materials research*, 2, 178-190.
- Lamela, M. J., Ramos, A., Fernández, P., Fernández-Canteli, A., Przybilla, C., Huerta, C., & Pacios, A. (2014). Probabilistic characterization of glass under different type of testing. *Procedia materials science*, 3, 2111-2116.
- Le, L. M., Ly, H. B., Pham, B. T., Le, V. M., Pham, T. A., Nguyen, D. H., ... & Le, T. T. (2019). Hybrid artificial intelligence approaches for predicting buckling damage of steel columns under axial compression. *Materials*, 12(10), 1670.
- Liu, Q., Huang, X., Liu, G., Zhou, Z., & Li, G. (2017). Investigation on flexural buckling of laminated glass columns under axial compression. *Engineering Structures*, 133, 14-23.
- Luible, A., & Crisinel, M. (2004). Buckling strength of glass elements in compression. *Structural engineering international*, 14(2), 120-125.
- Luible, A., & Crisinel, M. (2005). Plate buckling of glass panels. In *Proceedings of the International Conference Glass Processing Days 2005* (No. CONF, pp. 476-479).
- Ly, H. B., Desceliers, C., Minh Le, L., Le, T. T., Thai Pham, B., Nguyen-Ngoc, L., ... & Le, M. (2019). Quantification of uncertainties on the critical buckling load of columns under axial compression with uncertain random materials. *Materials*, 12(11), 1828.
- Miller, R. K., & Hedgepeth, J. M. (1979). The buckling of lattice columns with stochastic imperfections. *International Journal of Solids and Structures*, 15(1), 73-84.
- Mognato, E., Brocca, S., Barbieri, A., & del Vetro, S. S. (2017). Thermally processed glass: correlation between surface compression, mechanical and fragmentation test. *Glass Performance Days*, 8-11.
- Naess, A., Leira, B. J., & Batsevych, O. (2009). System reliability analysis by enhanced Monte Carlo simulation. *Structural safety*, 31(5), 349-355.
- Nurhuda, I., Lam, N. T. K., Gad, E. F., & Calderone, I. (2010). Estimation of strengths in large annealed glass panels. *International Journal of Solids and Structures*, 47(18-19), 2591-2599.
- Oh, J. K., Lee, J. J., & Hong, J. P. (2015). Prediction of compressive strength of cross-laminated timber panel. *Journal of wood science*, 61(1), 28-34.
- Oikonomopoulou, F., van den Broek, E. A. M., Bristogianni, T., Veer, F. A., & Nijssse, R. (2017). Design and experimental testing of the bundled glass column. *Glass Structures & Engineering*, 2(2), 183-200.
- Onkar, A. K., Upadhyay, C. S., & Yadav, D. (2007). Stochastic finite element buckling analysis of laminated plates with circular cutout under uniaxial compression.
- Pešek, O., Horáček, M., & Melcher, J. (2016). Experimental verification of the buckling strength of structural glass columns. *Procedia engineering*, 161, 556-562.
- Pisano, G., & Carfagni, G. R. (2017). Statistical interference of material strength and surface prestress in heat-treated glass. *Journal of the American Ceramic Society*, 100(3), 954-967.
- Santo, D., Mattei, S., & Bedon, C. (2020). Elastic Critical Moment for the Lateral-Torsional Buckling (LTB) Analysis of Structural Glass Beams with Discrete Mechanical Lateral Restraints. *Materials*, 13(11), 2492.
- Schillinger, D., Papadopoulos, V., Bischoff, M., & Papadrakakis, M. (2010). Buckling analysis of imperfect I-section beam-columns with stochastic shell finite elements. *Computational Mechanics*, 46(3), 495-510.
- Southwell, R. V. (1932). On the analysis of experimental observations in problems of elastic stability. *Proceedings of the Royal Society of London. Series A, Containing Papers of a Mathematical and Physical Character*, 135(828), 601-616.
- Strating, J., & Vos, H. (1973). Computer simulation of the ECCS buckling curve using a Monte-Carlo method. *HERON*, 19 (2), 1973.

Valarinho, L., Correia, J. R., Machado-e-Costa, M., Branco, F. A., & Silvestre, N. (2016). Lateral-torsional buckling behaviour of long-span laminated glass beams: Analytical, experimental and numerical study. *Materials & Design*, 102, 264-275.

Veer, F. A., Bristogianni, T., & Baardolf, G. (2018). A case study of apparently spontaneous fracture. *Glass Structures & Engineering*, 3(1), 109-117.